J Nanopart Res (2012) 14:758
DOI 10.1007/s11051-012-0758-z

RESEARCH PAPER

Aggregation and adhesion of gold nanoparticles in phosphate buffered saline

Shangfeng Du · Kevin Kendall · Panteha Toloueinia · Yasamin Mehrabadi · Gaurav Gupta · Jill Newton

Received: 9 August 2011 / Accepted: 25 January 2012 / Published online: 14 February 2012

Abstract In applications in medicine and more specifically drug delivery, the dispersion stability of nanoparticles plays a significant role on their final performances. In this study, with the use of two laser technologies, dynamic light scattering (DLS) and nanoparticle tracking analysis (NTA), we report a simple method to estimate the stability of nanoparticles dispersed in phosphate buffered saline (PBS). Stability has two features: (1) self-aggregation as the particles tend to stick to each other; (2) disappearance of particles as they adhere to surrounding substrate surfaces such as glass, metal, or polymer. By investigating the effects of sonication treatment and surface modification by five types of surfactants, including nonylphenol ethoxylate (NP9), polyvinyl pyrrolidone (PVP), human serum albumin (HSA), sodium dodecyl sulfate (SDS) and citrate ions on the dispersion stability, the varying self-aggregation and adhesion of gold nanoparticles dispersed in PBS are demonstrated. The results showed that PVP effectively prevented aggregation, while HSA exhibited the best performance in avoiding the adhesion of gold nanoparticle in PBS onto glass and metal. The simple principle of this method makes it a high potential to be applied to other nanoparticles, including virus particles, used in dispersing and processing.

Keywords Nanoparticles · Aggregation · Adhesion · Dynamic light scattering · Nanoparticle tracking analysis · Nanomedicine

Introduction

The application of nanoparticles in biomedicine is increasing rapidly and offers excellent prospects for the development of new non-invasive strategies for the diagnosis and treatment of cancer (Barreto et al. 2011). Significant advances have been made in synthetic methodology for nanoparticles (Lavik and von Recum 2011), such that it is now possible to prepare a variety of nanoparticles with highly controlled size, shape, surface charge and physicochemical characteristics, and to decorate their surfaces with polymers and bioactive molecules in order to improve biocompatibility and achieve active targeting (Cho et al. 2011). However, there is still a big concern regarding the safety of nanoparticles and the way they are treated in the regulatory process (Sekhon and Kamboj 2010). In applications, good dispersion and stability of nanoparticles, which are easily degraded during processing, significantly affect the final therapeutic performance. For example, the presence of aggregates in a protein

Electronic supplementary material The online version of this article (doi:10.1007/s11051-012-0758-z) contains supplementary material, which is available to authorized users.

S. Du (✉) · K. Kendall · P. Toloueinia · Y. Mehrabadi · G. Gupta · J. Newton
School of Chemical Engineering, University of Birmingham, Edgbaston, Birmingham B15 2TT, UK
e-mail: s.du@bham.ac.uk

formulation compromises product quality and may lead to unwanted immunogenicity (Schellekens 2002). In another case, nanoparticles smaller than 100 nm in diameter have been suggested to be ideal for cancer therapy (Gullotti and Yeo 2009) because of their favorable biodistribution and clearance/accumulation behavior (Alexis et al. 2008). Heavy aggregation might lead to serious toxicity. At present, very few nanoparticle types have achieved Food and Drug Administration (FDA) approval for use in cancer therapy. The detailed characterization of the materials is essential in all areas of nanotoxicology. In the coming years, significant progress is expected in improving our understanding of the basic physico-chemical characteristics, including aggregation and adhesion, that determine nanoparticle activity (2011).

Among the candidate materials, gold nanoparticles are receiving considerable attention, mainly because their properties lend themselves to multiple applications, such as labeling, delivery, heating, and sensing (Boisselier and Astruc 2009; Cho et al. 2011). Gold nanoparticles are made by simple reduction of metal salt precursors with reducing agents under controlled conditions, in either water or organic solvents. The conventional methods for the synthesis of gold nanoparticles are the citrate reduction of $HAuCl_4$ in water and the Brust–Schiffrin method (Zhou et al. 2009), in which thiol ligands are used to stabilize the nanoparticles by controlled binding to the surfaces of the particles.

Today, one of the most commonly used techniques for particle size analysis of nanoparticles and protein aggregates is dynamic light scattering (DLS). DLS is one of the most user-friendly techniques, and it yields relatively accurate and consistent results that can be obtained in a short period of time (Bootz et al. 2004). Therefore, DLS has become the preferred technique to determine the size of nanoparticles. Despite being a powerful and accessible tool, DLS is also known to have several drawbacks, which are mainly inherent to the principles of the technique. One of them is that this technique is very sensitive to the presence of large particles. This can be an advantage if the purpose is to detect small amounts of large particles, but it can be a major drawback for accurate size determination. Dust particles or small amounts of large aggregates can impede the size determination if the main component exhibits a distinctly smaller size (Berne and Pecora 2000).

Nanoparticle tracking analysis (NTA), also known as NanoSight, was originally developed by Carr and his colleagues to measure particle size (Malloy and Carr 2006). The instrument has been used to detect many different nanoparticle species (Du et al. 2010), and also to measure very small adhesion forces (Kendall et al. 2009, 2010b). The method is based on a laser illuminated microscopical technique, in which Brownian motion of nanoparticles in the scattering laser beam in liquid is analyzed in real time by a computer controlled charge-coupled device (CCD). With this method, each particle can be simultaneously but separately visualized and tracked, making the particle concentration directly measurable. A critical evaluation undertaken by Filipe et al. (2010) showed that this technique is very accurate for sizing both monodisperse and polydisperse samples and has a substantially better peak resolution than DLS, proving to be very suitable for analyzing nanoparticles and their aggregates.

In this study, with the help of DLS and NTA techniques, the effects of sonication treatment and surface modification on the stability of 40 nm gold nanoparticles dispersed in phosphate buffered saline (PBS) and water are investigated. Based on the results obtained, a novel method to estimate the aggregation and adhesion of nanoparticles is reported.

Materials and methods

Materials

All chemicals were used as received without further purification. All aqueous solutions were prepared using nanopure water (18.2 MΩ cm) from a Millipore water system. Gold colloid with a mean diameter of 41.5 nm and coefficient of variation (CV) <8% was purchased from BB International, UK. The colloid was prepared from gold chloride reduced by sodium citrate with a precursor concentration of 0.01%. PBS at pH 7.4 was made by dissolving one PBS tablet (Sigma-Aldrich) into 200 mL of water. Five surface modification agents were used as received from Sigma-Aldrich: nonylphenol ethoxylate (NP9), polyvinyl pyrrolidone (PVP, average M_w 40,000), human serum albumin (HSA, ≥97% lyophilized powder, wt 66,478 Da), sodium dodecyl sulfate (SDS, ≥99.0%), and sodium citrate (≥99.0%).

Sonication treatment

The sonication treatment was done in an ultrasound bath (Langford Sonomatic 1000, 33 kHz, UK). The sample solution was put in a 20 mL polystyrene bottle covered with cap and the operation was done for a set time at room temperature. In sonication treatment, every half an hour the ultrasound bath was re-filled with fresh tap water to avoid the possible influence from hot water. After treatment, the solution was immediately filled into DLS cuvette or injected into NTA for measurement.

Surface modification

Before mixing with gold nanoparticles, surface modification agents were first diluted to a certain concentration with water and stored in refrigerator for 10 h. Typically, for the preparation of a 10 mL PBS solution sample with 10 ppm HSA and gold nanoparticles with a dilution times of 100, HSA lyophilized powder was first diluted for 1,000 times with water to make 1,000 ppm HSA solution. Then, 100 μL 1,000 ppm HSA solution and 100 μL gold colloid were mixed with a *Whirlimixer* brand vortex mixer for 30 s in a 20 mL polystyrene bottle covered with cap at room temperature, followed by adding 9.8 mL PBS into the mixture and mixing for another 30 s. Then, the sample was immediately moved to sonication treatment or filled into DLS cuvette or injected into NTA for measurement.

Dynamic light scattering

DLS measurements were performed with a Malvern HPPS (High Performance Particle Sizer, UK) system equipped with a 3.0 mW, 33 nm He–Ne laser and operating at an angle of 173°. The software used to collect and analyze the data was Dispersion Technology Software version 4.0 from Malvern. The samples used for DLS measurement were diluted from the purchased gold colloid for 100 times by water or PBS. 2 mL of each sample was measured in 12 mm square polystyrene cuvettes (SARSTEDT, Germany) with a path length of 10 mm. The measurements were made at a controlled temperature of 25 °C after equilibrium duration of 3 min. For each sample, 15 runs of 10 s were performed, with three repetitions for all samples. The intensity size distribution was obtained from the autocorrelation function using the "general purpose mode."

Nanoparticle tracking analysis

NTA measurements were carried out with a NanoSight LM10 system (NanoSight, Amesbury UK), equipped with a sample chamber with a 640 nm red laser and a Viton fluoroelastomer O-ring. The samples used for NTA measurement were diluted from the purchased gold colloid by 200 times with water or PBS. The samples were injected into the sample chamber with 2.5 mL sterile syringes (SD Plastidek, Spain) until the liquid reached the tip of the nozzle. All measurements were performed at room temperature. The software used for capturing and analyzing the data was the NTA 2.0 Build 127. The samples were measured for 40 s with manual shutter and gain adjustments, but the parameters were kept at the same for all comparison samples. The "single shutter and gain mode" was used to capture all samples. Three measurements were undertaken for each sample. The details of particle number counting are described in our previous study (Du et al. 2010). Typically, the mean particle number per frame was counted from 36 frames which were taken from the videos of the three measurements for each sample. The particle numbers were counted by the white scattered light spots which could be indentified clearly in each frame. The error bars displayed on the NTA number counting graphs were obtained by the standard deviation of the total 36 frames of each sample.

Results and discussion

PBS is a buffer solution frequently utilized as stimulated human body fluid in biological research. It is a water-based salt solution consisting phosphate buffer, sodium chloride, and potassium chloride (0.01, 0.137, and 0.0027 M in this experiment, respectively). When nanoparticles are dispersed in PBS, the relatively high ionic strength could cause particle aggregation, thus changing the dispersion behavior of nanoparticles which could lead both to destabilization and adhesion to surrounding substrates.

Because of the van der Waals forces acting at the surfaces of nanoparticles, they can adhere to the substrates, e.g., glass or metal surfaces used in many

research investigations (Kendall et al. 2010a). Such adhesion has been investigated for various nanoparticle types, e.g., silver nanoparticles, carbon nanotubes (CNT) with cells, and other organic or inorganic nanoparticles (Sungchul and Daniel 2010), but little research has been carried out on nanoparticles dispersed in PBS. During NTA measurements, the sample is in contact with glass, stainless steel, a Viton fluoroelastomer O-ring, and nylon tubing in the sample chamber. The high adhesion energy on the surface of the nanoparticles in PBS could result in the sticking of nanoparticles to these substrates. Thus, it is possible for us to evaluate the adhesion from their stability in the NTA sample chamber by counting the particle number decreasing with time for nanoparticles dispersed in PBS, considering the aggregation effect which could be detected by DLS where very little sticking exists between the nanoparticles and the inert polystyrene cuvette used (Lee et al. 2007; Kobayashi et al. 2007; Tian et al. 2010, 2011).

Figure 1 shows the particle counting with time in the NTA for the 40 nm gold nanoparticles dispersed in water and PBS. Gold nanoparticle dispersed in PBS suffered a fast decline and more than 80% particles disappeared after only 30 min. While in water, the situation was much better. A much higher particle number per frame was obtained and no obvious drop observed even after 120 min. The small particle counting number in PBS confirms the ionic strength in PBS accelerate the aggregation process between nanoparticles, and the fast drop indicates a strong adhesion of nanoparticles to the chamber surfaces in the NTA sample cell.

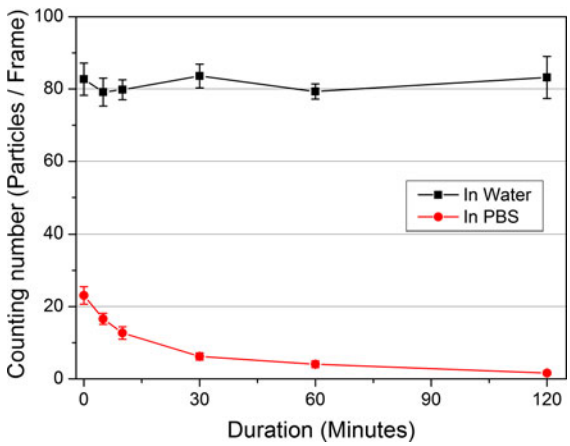

Fig. 1 NTA particle counting with time for 40 nm gold nanoparticles dispersed in water and PBS

Effects of sonication treatment

One of the problems of nanoparticle measurement is the long time required for the distribution of aggregate sizes to reach an equilibrium value. It was shown that about 5 days was necessary for a dispersion of 60 nm oxide particles to return to its normal value after a sudden disturbance of stability (Kendall et al. 2010a). Although it has been shown that a stable colloid may be largely composed of single particles, 10% may be doublet aggregates, 1% may be triplets and smaller proportions may be aggregates of up to 30 particles. In this study, sonication treatment was employed as a tool to improve the dispersion of nanoparticles with or without surfactants in liquids. It has been known that an optimized treatment duration can help dispersing and make the suspension more uniform, but too long a sonication time could also lead to ultrasound-driven aggregation (Zhong et al. 2006; Radziuk et al. 2010). To obtain the optimum sonication time, the particle size distributions were measured by DLS after various sonication durations and the results are shown in Fig. 2. It can be seen that the best performance was obtained with sonication of 5–10 min for gold nanoparticles dispersed in water. The peak position moved to a smaller size demonstrating some aggregates are broken. Too long a treatment duration (30 min) results in more aggregates and the peak position shifting to large size. In PBS, the sonication treatment provides more chance for nanoparticles to contact with the ions, and then more aggregation was obtained as expected, as shown in Fig. 2b. The longer treatment duration made the particle size distribution shift to a much larger size. For each sonication treatment duration, a peak position near 90–100 nm was obtained for nanoparticles dispersed in PBS, which is much larger than that of 40–60 nm in water, indicating the significant aggregation within the system.

The effect of sonication treatment was also checked by NTA. Due to the heavy aggregation and adhesion of gold nanoparticles in PBS, NTA particle counting on the plain gold nanoparticles was only carried out on the water sample and the results are shown in Fig. 3. A maximum value was obtained for the sample with

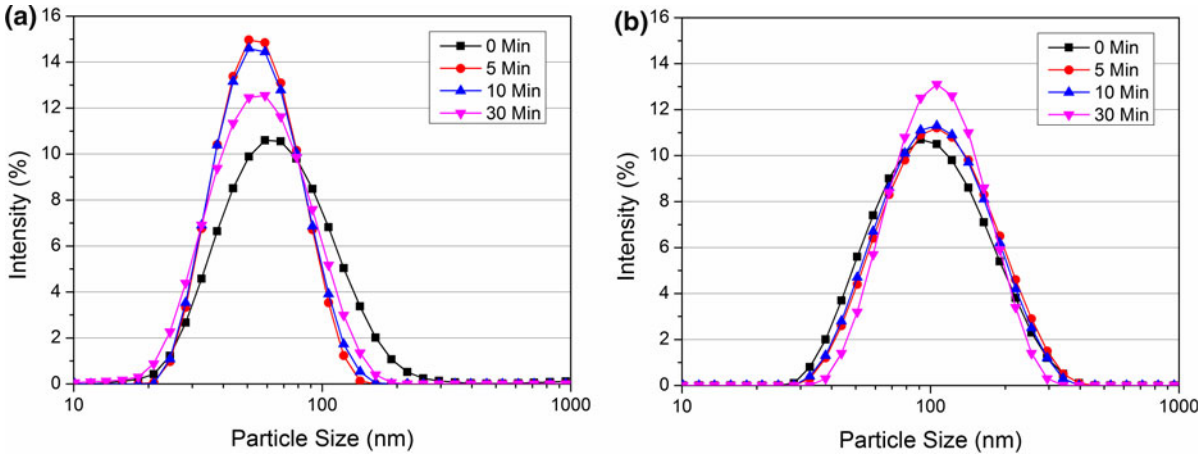

Fig. 2 Dynamic light scattering measurements showing effects of sonication treatment duration on gold nanoparticles dispersed in water (**a**) and PBS (**b**)

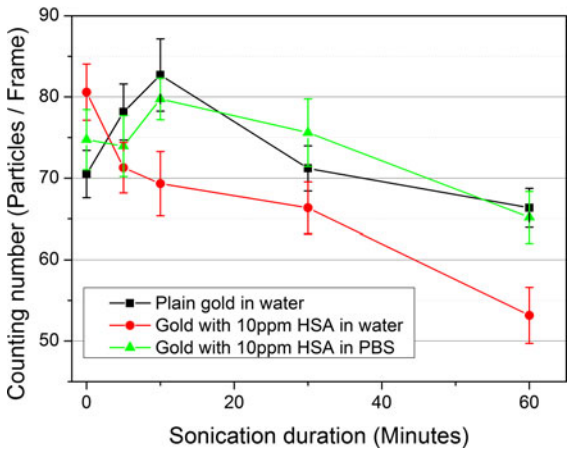

Fig. 3 NTA particle counting number with sonication time for plain gold nanoparticles dispersed in water, and surface modified with 10 ppm HSA in water and PBS

10 min sonication treatment and a longer time result in a continuing decrease to the particle counting number.

To check the sonication effect, treatment was also performed to surface-modified gold nanoparticles dispersed in water and PBS, and the results are also shown in Fig. 3. Surfactants were added to prevent the self-aggregation of gold nanoparticles. 10 ppm HSA was used as surfactant here. The figure indicates that the surface modification bring a quite different behavior to gold nanoparticles in water, and the NTA particle counting number keep decreasing with treatment duration. While, in PBS, the HSA-modified gold nanoparticles exhibited a quite similar situation to plain gold nanoparticles in water, and 10 min sonication treatment led to the maximum particle counting number. The poor performance of HSA for modifying gold nanoparticles in water may come from the protein feature of HSA. This result also demonstrates that sonication treatment is strong enough to induce ultrasound-driven aggregation even for the surface-modified gold nanoparticles. Hence, a sonication treatment duration of 10 min was selected for all following experiments to investigate the self-aggregation and adhesion of gold nanoparticles in PBS.

Effects of surfactants on gold nanoparticle behavior in PBS

Five types of surfactant were tested in this study: the non-ionic surfactant NP9, polymer PVP, a water-soluble protein HSA, the anionic surfactant SDS, and citrate ions.

Nonylphenol ethoxylate (NP9)

DLS result for the samples with various NP9 concentrations are shown in Fig. 4. It can be observed that the sample with 1 ppm NP9 has an obvious peak shifting with time, but this shifting is not apparent for the samples with 5 or 10 ppm NP9. The comparison of various concentrations (Fig. 4d) demonstrates that the addition of NP9 obviously reduces the aggregation of gold nanoparticles in PBS, in comparison with the plain gold without any surfactants. It also shows that

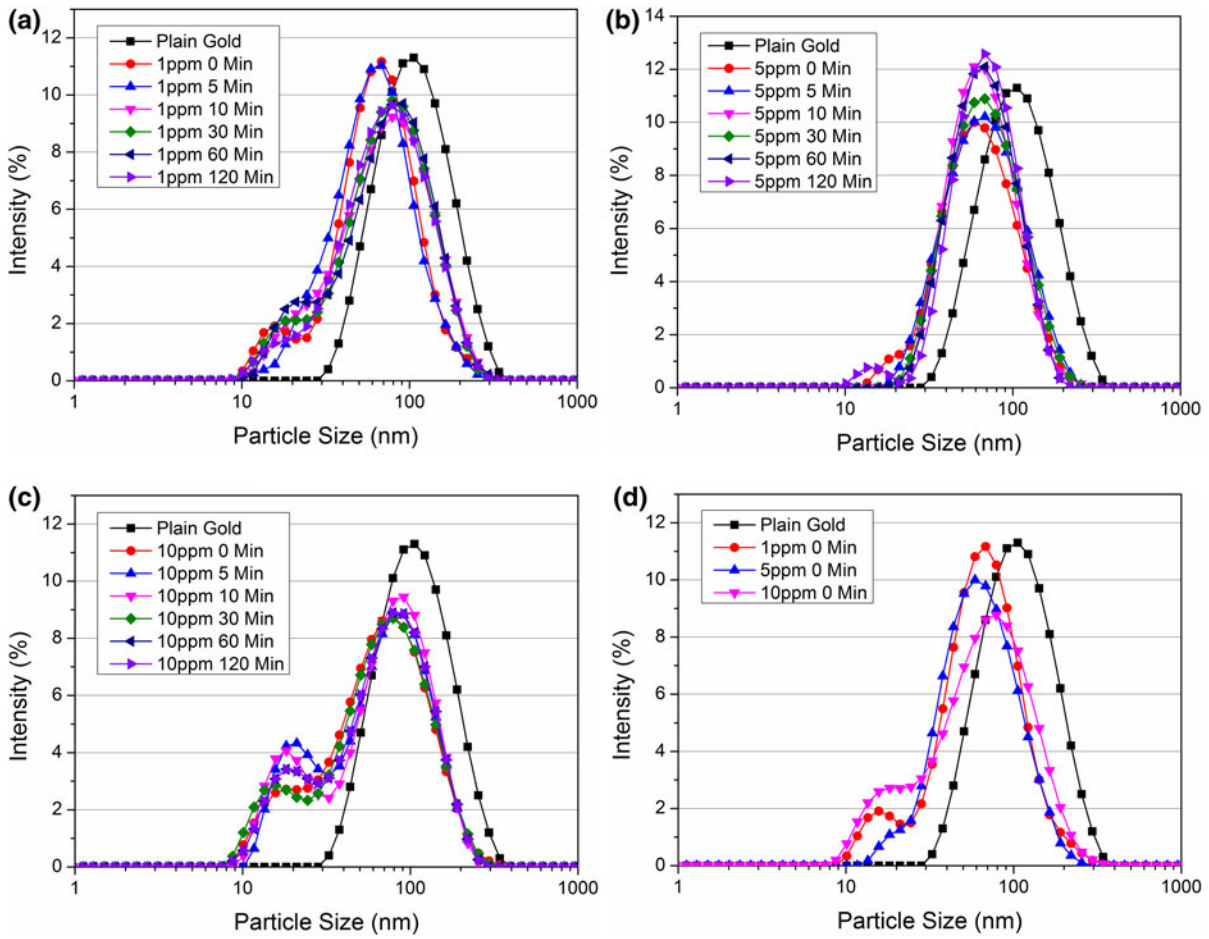

Fig. 4 DLS measurements showing effects of NP9 concentration on 40 nm gold nanoparticles dispersed in PBS: **a** 1 ppm NP9, **b** 5 ppm NP9, **c** 10 ppm NP9, and **d** their comparison at 0 min with various concentrations

the sample with 5 ppm NP9 has the smallest peak position and a high NP9 concentration of 10 ppm results in a peak shifting toward large side, indicating more aggregates are introduced. There is also a small peak at 10–20 nm in each DLS particle size distribution plot, which might come from NP9 micelles formed in liquid.

NTA result for the samples with various NP9 concentrations are shown in Fig. 5. With NP9 concentration at 1 ppm, the gold nanoparticle number shown by NTA counting keeps decreasing in solution with time. It has a quite similar trend to the plain gold without surfactant, demonstrating the poor effect of NP9 at this low concentration. Increasing the NP9 concentration to 5 ppm, the aggregation decreases (Fig. 5c), and the particle counting number increase to a much higher value of about 87 particles/frame for the fresh sample, but still declines very fast. After increasing NP9 concentration to 10 ppm, this decline becomes very slow and the particle counting number is nearly stable within 120 min. However, the total particle counting number for a fresh sample with 10 ppm NP9 is only about 60, which is much smaller than that at a low concentration of 5 ppm. It can be seen that there is a large aggregation peak formed at ca. 90–120 nm for particle size distribution (Fig. 5d), which is in line with the peak shifting to large size observed in DLS (Fig. 4d). The formation of these aggregates reduces the total particle number leading to a smaller counting number at Fig. 5a. In fact, this peak can be found even at a low concentration as 1 ppm, where this peak appeared as only a small shoulder at ca. 100 nm on the particle size distribution plots. Hence, the decline on the particle counting number at

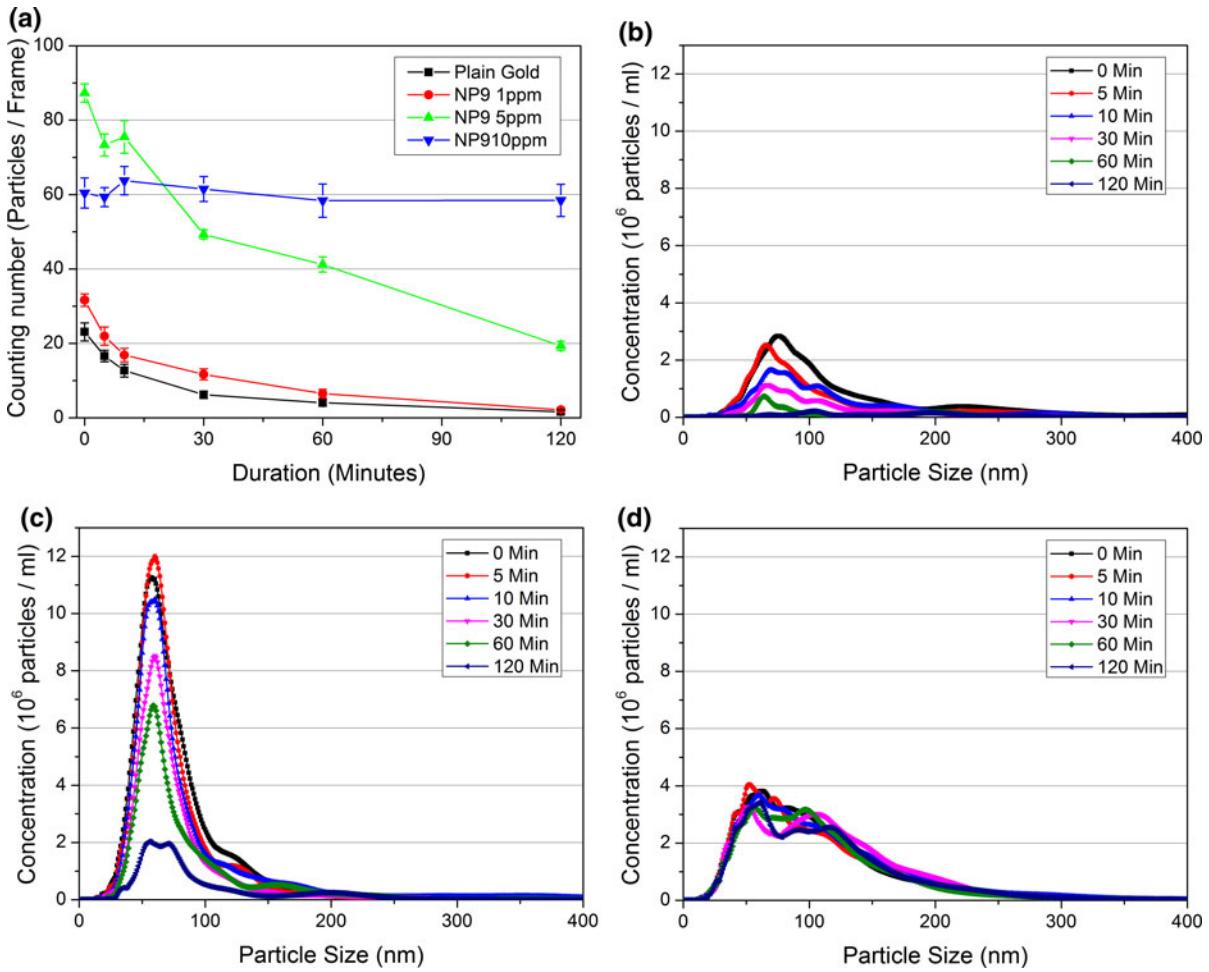

Fig. 5 NTA results for 40 nm gold nanoparticles modified with various concentrations of NP9 in PBS: **a** particle counting number, **b** 1 ppm NP9, **c** 5 ppm NP9, and **d** 10 ppm NP9

low concentration of 1 or 5 ppm also comes partly from the developing formation of aggregates. The possible reason for the formation of these special aggregates might come from the 9 ethoxy groups in NP9. If 2–9 of total 9 ethoxy groups each takes one single 41.5 nm gold nanoparticle, they formed special aggregates will consist from 2 to 9 single gold nanoparticles, exhibiting an equivalent hydrodynamic diameter from 62 to 148 nm (Takayasu and Galembeck 1998). This size range is in accord with the observation in Fig. 5d.

Here, we can find that all small peaks at 10–20 nm in all DLS particle size distributions (Fig. 4) are below the measurement size range and cannot be detected by NTA. Howevere, DLS failed to show simultaneously the two peaks from single monodisperse particles and aggregates, and only a large middle peak near aggregate size is observed. This biasing to large particles has been evaluated by Filipe et al. (2010) as a serious drawback in characterizing protein aggregations by DLS technique in comparison with NTA.

Polyvinyl pyrrolidone

Similar to NP9, as a polymer, PVP is commonly used as dispersing agent for nanoparticles. The good dispersing effect of PVP in preventing the aggregation of gold nanoparticle in PBS was also confirmed by the DLS measurement results as shown in Fig. 6. At a concentration at 10 ppm, a narrow particle size

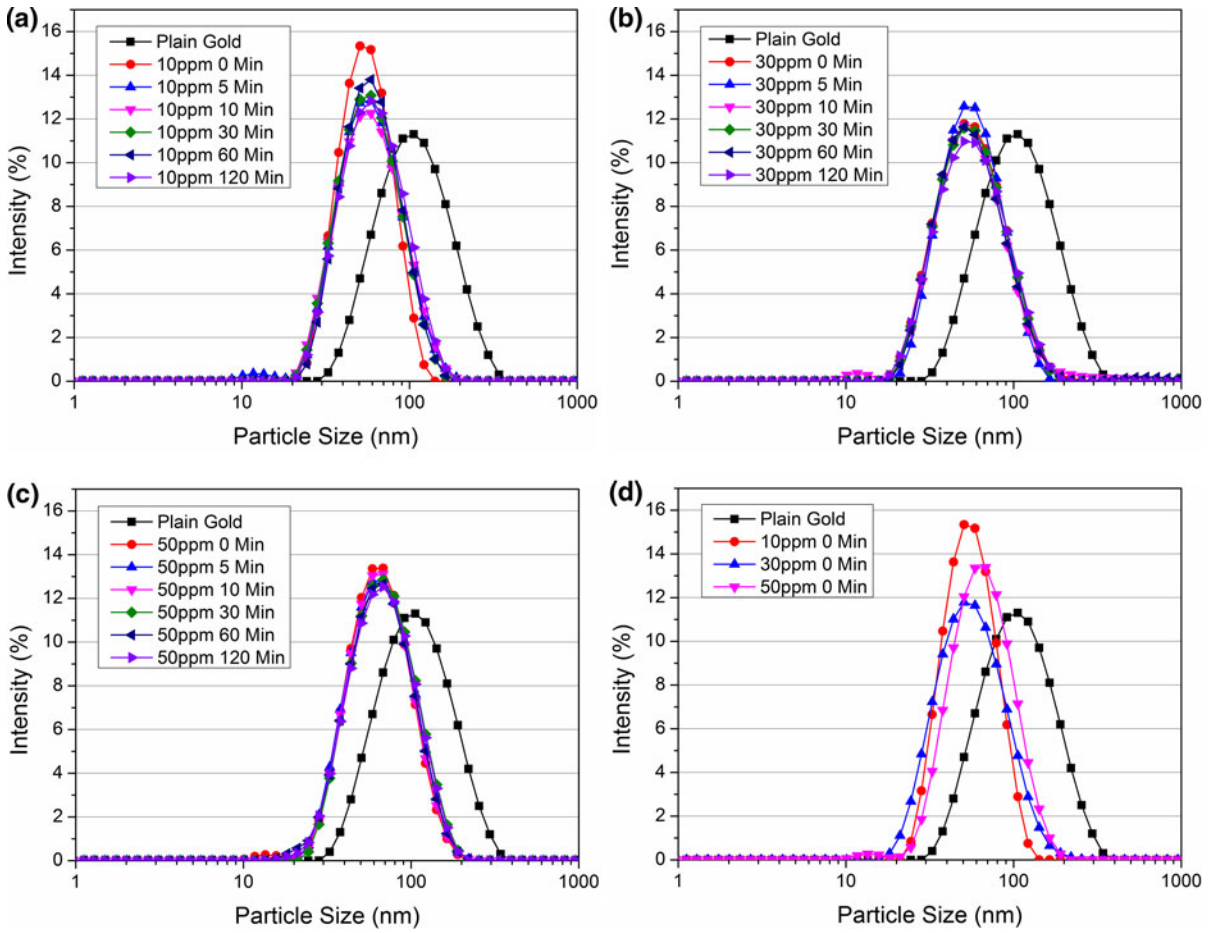

Fig. 6 DLS measurements showing effects of PVP concentration on 40 nm gold nanoparticles dispersed in PBS: **a** 10 ppm PVP, **b** 30 ppm PVP, **c** 50 ppm PVP, and **d** their comparison at 0 min with various concentrations

distribution is obtained, and only a small change happened with time to the fresh sample. The sample with 30 ppm PVP is nearly stable and no obvious peak shifting is detected. With 50 ppm PVP, there is almost no change with the particle size distribution within 120 min. The comparison of the samples with various PVP concentrations (Fig. 6d) shows a better performance of PVP than NP9 in stabilizing gold nanoparticles in PBS, but a slight shifting of peak position to large size is still observed to the sample with 50 ppm PVP, indicating a lower PVP concentration as 30 ppm might be better in this application.

Figure 7 shows the NTA results of gold nanoparticles dispersed in PBS with various PVP concentrations. At the concentration of 10 ppm, the particle counting number detected by NTA is very low (Fig. 7a) and the peak intensity for particle size distribution decreases very fast (Fig. 7b), although the aggregate ratio is not large and a narrow and sharp peak is obtained on the particle size distribution. After 60 min, nearly all particles are disappeared. The NTA measurement frames are shown in Fig. S1 in the Supplementary material for the sample with 10 ppm PVP at various time durations. Increasing the PVP concentration slowed this decline, but even at 50 ppm the sample was still not stable although a large particle counting number was obtained to the fresh sample. This could also be seen from the decreasing particle counting number with time shown in Fig. 7a. The narrow particle distribution indicates this decline should come from the heavily sticking of nanoparticles on the surround surfaces in the NTA sample cell.

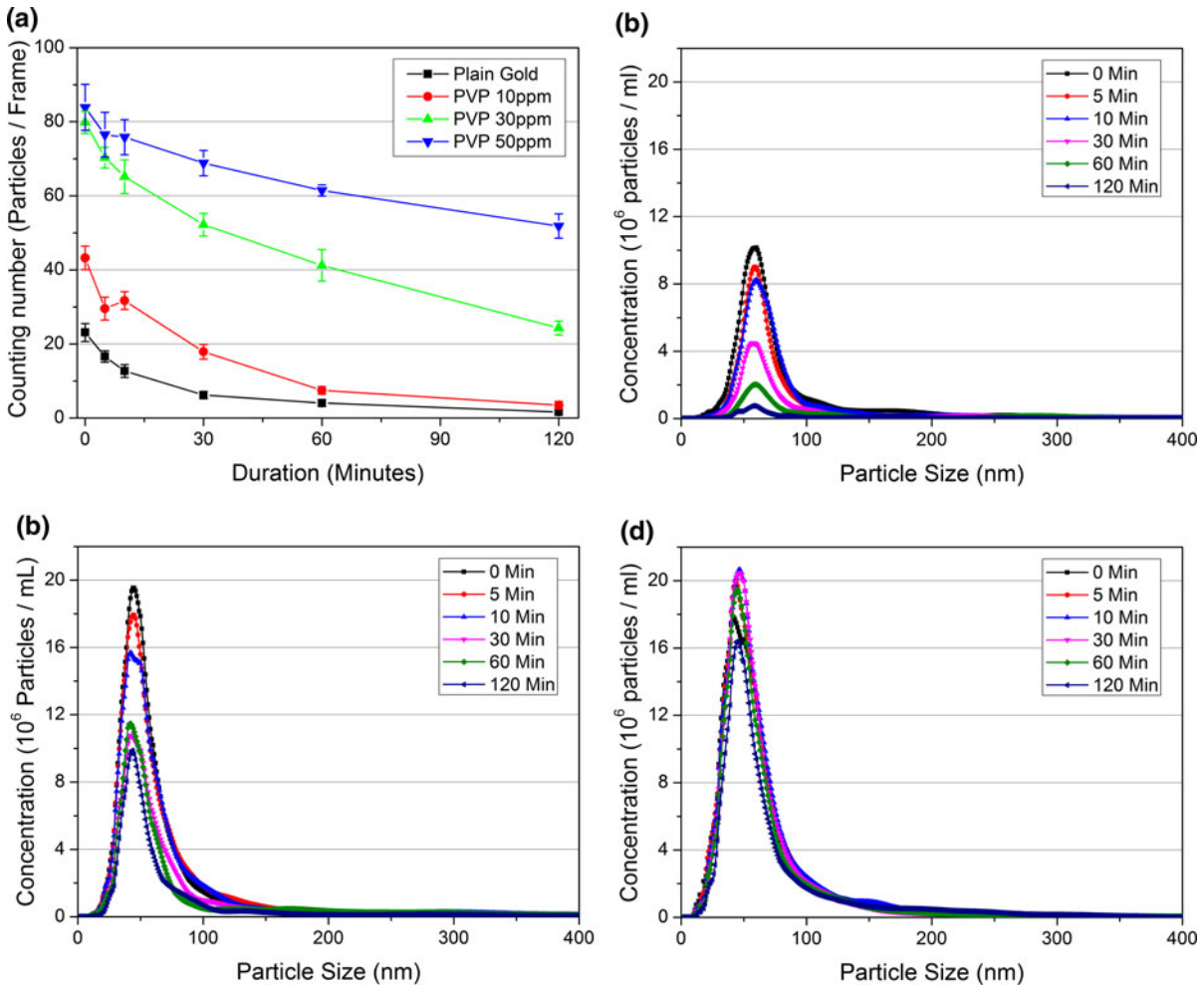

Fig. 7 NTA results for 40 nm gold nanoparticles modified with various concentrations of PVP in PBS: **a** particle counting number, **b** 10 ppm PVP, **c** 30 ppm PVP, and **d** 50 ppm PVP

Considering the stable particle size distributions obtained from DLS measurements (Fig. 6), it can be confirmed that the particle counting decline is not caused by nanoparticle aggregation, but the strong sticking to the inside chamber surfaces. A short movie on the sample with 30 ppm PVP was enclosed in the Supplementary material, clearly showing this sticking. In fact, after leaving the sample with 50 ppm PVP in NTA cell overnight, we found that all particles had disappeared from the liquid and a layer of gold nanoparticles was formed on the glass surface. This layer even cannot be removed by simply scrubbing with ethanol and acetone, indicating strong adhesion of the PVP-modified gold nanoparticles with glass surface.

Human serum albumin

HSA is an abundant plasma protein found in human body. It is obtained from the expired blood plasma and totally compatible with the human body (He and Carter 1992). The stabilizing effect of HSA for gold nanoparticles in PBS is shown by the DLS measurement results in Fig. 8. It can be seen that even at 1 ppm, the sample is nearly stable and no large peak shifting after 120 min. The comparison of the samples with three different HSA concentrations shows a slight shifting on peak to the small size when increasing the HSA concentration from 1 to 10 ppm (Fig. 8d). The perfect peak shape and stability were achieved for the sample with 10 ppm HSA, indicating the high

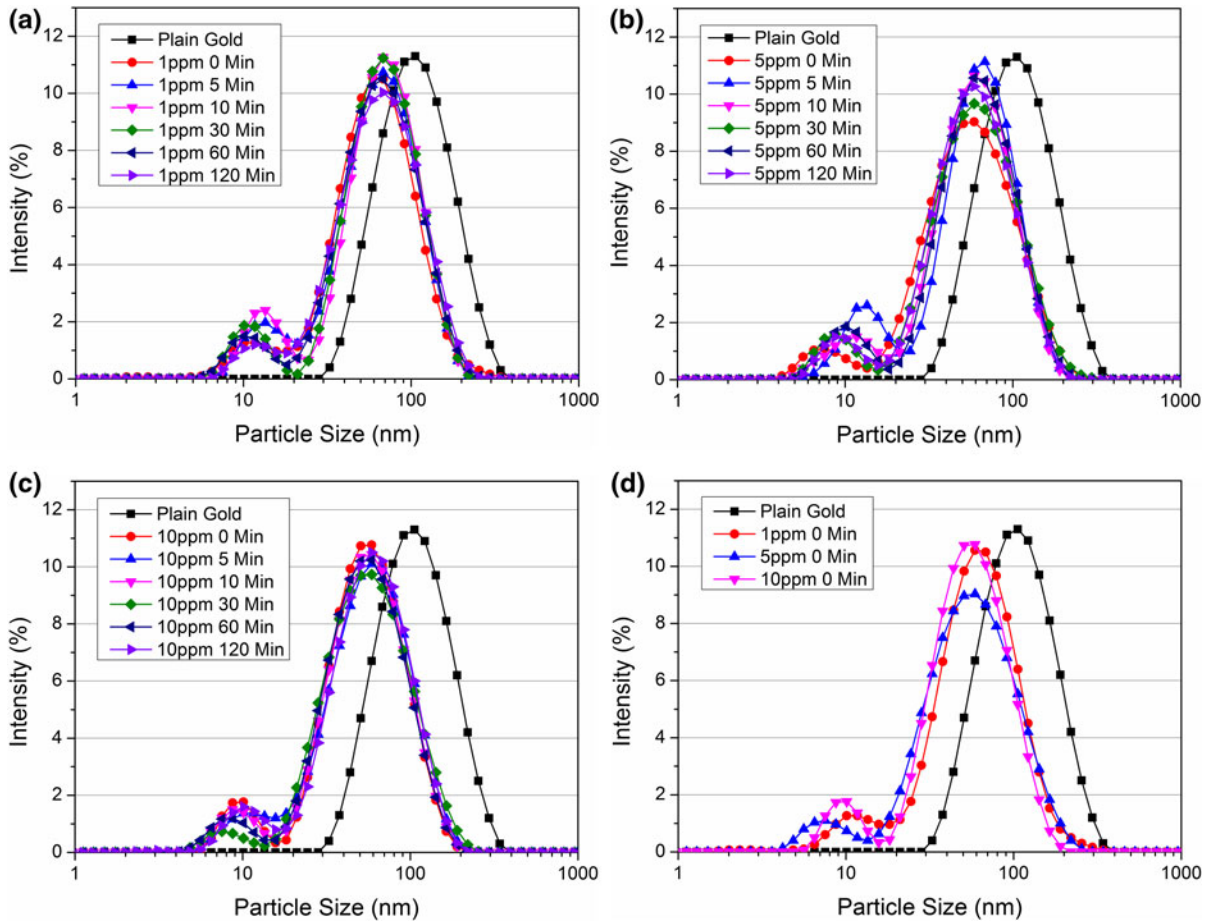

Fig. 8 DLS measurements showing effects of HSA concentration on 40 nm gold nanoparticles dispersed in PBS: **a** 1 ppm HSA, **b** 5 ppm HSA, **c** 10 ppm HSA, and **d** their comparison at 0 min with various concentrations

efficiency of HSA in preventing the aggregation of gold nanoparticles in PBS. The small peak between 4 and 20 nm comes from the HSA molecular (He and Carter 1992).

The surface modification effect of HSA for gold nanoparticles in PBS is also shown by NTA measurement results (Fig. 9). A low HSA concentration of 1 ppm shows very little effect, but the performance improves with the HSA amount. At a concentration of 10 ppm, a perfect monodisperse type particle size distribution was achieved. The particle counting number shows a high value near 80 particles/frame (Fig. 9a), although it is still a little lower compared to the fresh sample with 5 ppm NP9, or with 30 or 50 ppm PVP samples. The important point is that this sample exhibits a very good stability, and little decline has been observed within 120 min. In this case, 10 ppm HSA can effectively prevent the aggregation and adhesion of gold nanoparticles, and can be used as a good surfactant for stabilizing gold nanoparticles in PBS. The small HSA molecular peak between 4 and 20 nm (Fig. 8) is below the detection limit of NTA and cannot be seen in Fig. 9.

Sodium dodecyl sulfate

Similar to PVP, SDS is also widely used as an ionic surfactant in stabilizing inorganic or metal nanoparticle dispersions. To check the performance of SDS on dispersing gold nanoparticle in PBS, a sample with 50 ppm SDS was measured and the DLS results are shown in Fig. 10a. It shows a heavy aggregation by the large peak positions over 100 nm. The continuing shifting of peak position with duration also

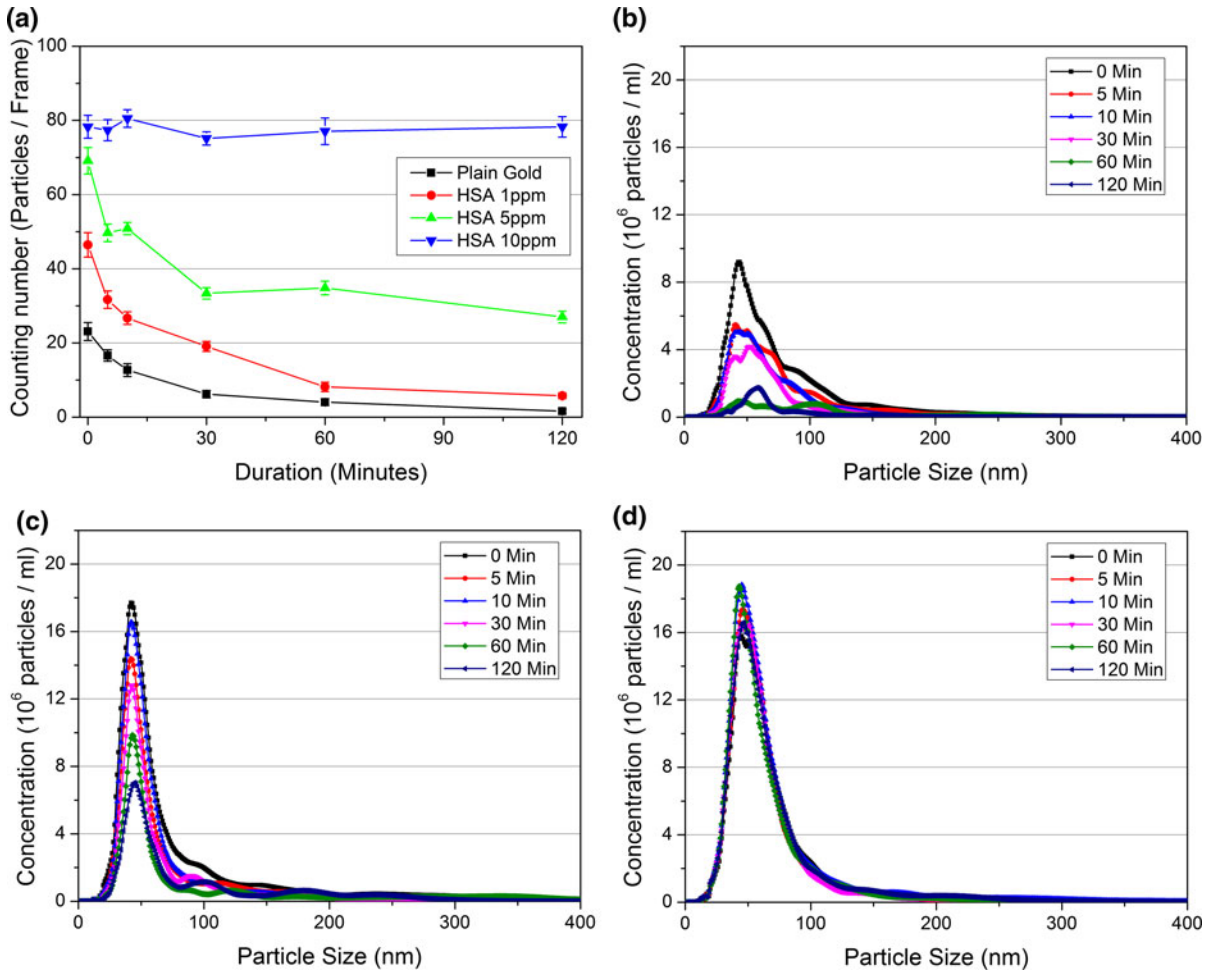

Fig. 9 NTA results for 40 nm gold nanoparticles modified with various concentrations of HSA in PBS: **a** particle counting number, **b** 1 ppm HSA, **c** 5 ppm HSA, and **d** 10 ppm HSA

demonstrates the poor stability even at this high surfactant concentration.

Figure 10b and c shows the NTA measurement results for the samples with SDS. The same results were obtained as in DLS measurement, even with a high concentration as 50 ppm, the aggregation can still not be eliminated. The small particle counting number and the fast decline with time indicate the poor stabilizing performance of SDS for gold nanoparticles in PBS.

Citrate ions

Citrate ions can effectively stabilizing gold nanoparticle in water. The citrate ions act as the reducing agent in nanoparticle preparation making this method very simple and convenient, because no other surfactants are necessary in the system. However, citrate stabilized gold in PBS showed poor dispersion. As shown in Fig. 11a, we can see that all profiles are quite similar or even worse compared with those samples stabilized with SDS. NTA measurement results for the samples with 50 ppm sodium citrate are shown in Fig. 11b and c. The same the results is obtained as in the DLS measurement, and an even worse stabilizing performance was found as compared with SDS.

In fact, the poor performance from SDS and citrate ions in stabilizing gold nanoparticles in PBS is as expected. The SDS and citrate ions will adsorb onto the nanoparticle surface leading to an increase on the electrostatic repulsive forces between nanoparticles. However, the high ionic strength in PBS will screen

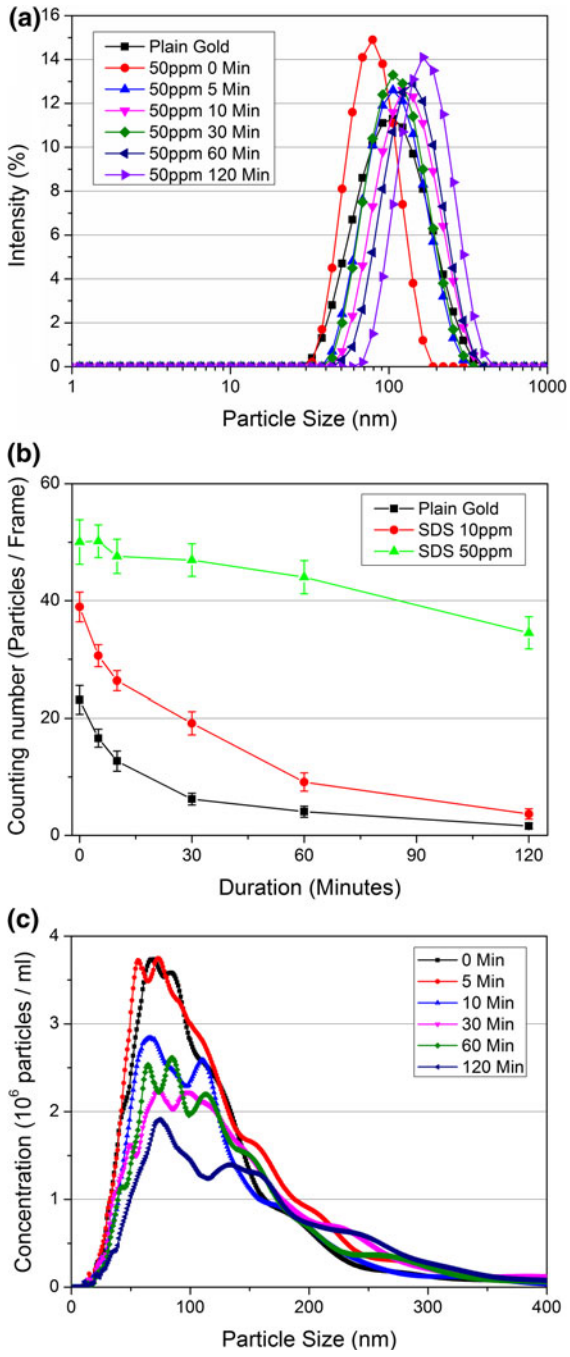

Fig. 10 DLS and NTA measurements showing stability effects of SDS on 40 nm gold nanoparticles dispersed in PBS: **a** DLS results for sample with 50 ppm SDS, **b** NTA particle counting number, and **c** NTA results for sample with 50 ppm SDS

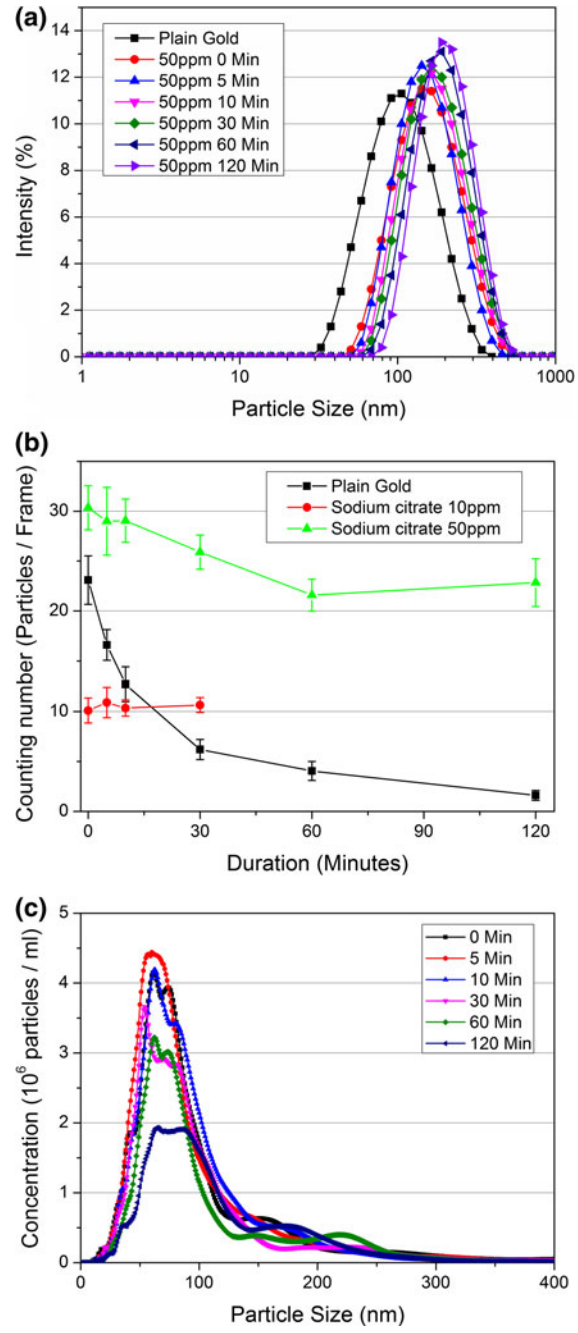

Fig. 11 DLS and NTA measurements showing stability effects of sodium citrate on 40 nm gold nanoparticles dispersed in PBS: **a** DLS results for sample with 50 ppm sodium citrate, **b** NTA particle counting number, and **c** NTA results for sample with 50 ppm sodium citrate

these repulsive forces rendering the stabilizers ineffective. While NP9 is much better than SDS and citrate ions here, but the large ratio of aggregates formed (Fig. 5d) is a big problem in applications. Although the high particle counting number for the fresh sample with 5 ppm NP9 (Fig. 5a) indicates the good ability of

this amount of NP9 in preventing the aggregation, but the fast decline number with time demonstrates this concentration is still far too low to avoid the adhesion of gold nanoparticles to the chamber surface and stop the sticking. In this case, NP9 is not a good surfactant for dispersing gold nanoparticles in PBS.

PVP is highly effective in dispersing gold nanoparticles in PBS and no large aggregates are formed in the concentration from 10 to 50 ppm. A very large particle counting number obtained for the fresh sample with 50 ppm PVP. However, the strong adhesion of PVP-modified gold nanoparticle surfaces leads to a heavy sticking to the chamber surfaces and thus resulting in a fast decline of nanoparticle number in PBS. In fact, the very strong adhesion of PVP with metal or glass surface has been frequently mentioned (Crespo-Quesada et al. 2011). It is this strong contact makes it a perfect surfactant to prevent the metal nanoparticles growing big and the particle aggregation in the synthesis and process, but also brings some problems. For example, when synthesizing Pt-nanowire electrocatalysts, this strong adhesion resulted in a large difficulty in getting rid of PVP from the prepared nanowire surface resulting in a poor catalytic performance (Lee et al. 2008). In this study, this strong adhesion effect causes a serious sticking of the modified gold nanoparticles to the chamber surface, resulting in a fast decline of nanoparticle number in liquid. In this case, care should be taken with the use of PVP when synthesizing nanoparticles for bio-applications. The strong adhesion will make the removing of the nanoparticle become very difficult. However, this property might be utilized to build the self-assembly gold nanoparticle layers on substrate surfaces, which are usually very difficult to achieve in water or organic solvent.

Compared with PVP, HSA is also highly effective to prevent the aggregation. At a concentration of 1 or 5 ppm, some aggregates can still be observed in particle size distribution plots as measured by NTA (Fig. 8b, c), and the sticking also cannot be stop effectively. However, at a high concentration as 10 ppm, the satisfied result was achieved. The aggregation is very little and the sample is highly stable within 120 min. This indicates HSA is highly useful in reducing the adhesion of gold nanoparticles in PBS and avoiding their sticking to glass or metal surfaces. In addition to the excellent biocompatible ability, HSA can be used as a perfect surfactant to stabilize gold nanoparticles for applications in bio-systems.

In our former research, we have shown that NTA can also be used to measure adenovirus, which can be easily characterized like normal nanoparticles in PBS (Du et al. 2010; Kendall et al. 2010b). Hence, the method described in this study has also the potential capacity to be used for the evaluation of the self-aggregation between viruses and their sticking to other tissue surfaces, from which methods might be found to accelerate the self-aggregation of virus to form a large aggregates, or cover the active sites on virus surface by other nanoparticles, or even to reduce the adhesion force of virus surfaces to decrease their chance of sticking to cell surfaces thus eliminating the toxicity of virus.

Conclusions

In this study, by using two nanoparticle measuring methods, NTA as a new characterization approach and DLS as a common particle sizing technique, a novel method was successfully developed to evaluate the aggregation and adhesion of gold nanoparticles dispersed in water and PBS. The effects of sonication treatment and surface modification by surfactants on the stability of 40 nm gold nanoparticles in PBS were investigated in detail. The results showed an optimized sonication time of 10 min to reach equilibrium for plain gold nanoparticles in water or HSA-modified gold nanoparticles in PBS. A longer treatment duration led to ultrasound-driven aggregation of nanoparticles. NTA and DLS results demonstrated that 10 ppm HSA can be selected as an effective surfactant to stabilize 40 nm gold nanoparticles in PBS. It could prevent both the self-aggregation of nanoparticles and their adhesion to metal or glass surfaces. Although PVP exhibited a good performance in preventing aggregation, strong adhesion resulted in a heavy sticking to metal and glass substrates limiting its application. 10 ppm NP9 could also effectively reduce the adhesion, but gold nanoparticle aggregates were formed at a size range of 90–120 nm. SDS and citrate ions performed much worse in stabilizing gold nanoparticles in PBS. The results demonstrate that this novel method based on DLS and NTA can be used efficiently to estimate the aggregation and adhesion of nanoparticles in liquids. It should be possible to extend this application to other nanoparticles, including virus particles, used in dispersing and processing.

Acknowledgments This study was supported by a Research Fellowship from Science City Research Alliance (SCRA) awarded to Dr Du.

References

(2011) The dose makes the poison. Nat Nanotechnol 6(6):329

Alexis F, Pridgen E et al (2008) Factors affecting the clearance and biodistribution of polymeric nanoparticles. Mol Pharm 5(4):505–515

Barreto JA, O'Malley W et al (2011) Nanomaterials: applications in cancer imaging and therapy. Adv Mater 23(12): H18–H40

Berne BJ, Pecora R (2000) Dynamic light scattering: with applications to chemistry, biology, and physics. Dover Publications, Mineola

Boisselier E, Astruc D (2009) Gold nanoparticles in nanomedicine: preparations, imaging, diagnostics, therapies and toxicity. Chem Soc Rev 38(6):1759–1782

Bootz A, Vogel V et al (2004) Comparison of scanning electron microscopy, dynamic light scattering and analytical ultracentrifugation for the sizing of poly(butyl cyanoacrylate) nanoparticles. Eur J Pharm Biopharm 57(2):369–375

Cho EC, Zhang Q et al (2011) The effect of sedimentation and diffusion on cellular uptake of gold nanoparticles. Nat Nanotechnol 6(6):385–391

Crespo-Quesada M, Andanson J-M et al (2011) UV-ozone cleaning of supported poly(vinylpyrrolidone)-stabilized palladium nanocubes: effect of stabilizer removal on morphology and catalytic behavior. Langmuir 27(12): 7909–7916

Du S, Kendall K et al (2010) Measuring number-concentrations of nanoparticles and viruses in liquids on-line. J Chem Technol Biotechnol 85(9):1223–1228

Filipe V, Hawe A et al (2010) Critical evaluation of nanoparticle tracking analysis (NTA) by nanosight for the measurement of nanoparticles and protein aggregates. Pharm Res 27(5): 796–810

Gullotti E, Yeo Y (2009) Extracellularly activated nanocarriers: a new paradigm of tumor targeted drug delivery. Mol Pharm 6(4):1041–1051

He XM, Carter DC (1992) Atomic structure and chemistry of human serum albumin. Nature 358(6383):209–215

Kendall K, Dhir A et al (2009) A new measure of molecular attractions between nanoparticles near kT adhesion energy. Nanotechnology 20(27):275701

Kendall K, Kendall M et al (2010a) Adhesion of cells, viruses and nanoparticles. Springer, New York

Kendall K, Du S et al (2010b) Virus concentration and adhesion measured by laser tracking. J Adhes 86(10):1029–1040

Kobayashi Y, Tadaki Y et al (2007) Deposition of gold nanoparticles on polystyrene spheres by electroless metal plating technique. J Phys Conf Ser 61:582–586

Lavik E, von Recum H (2011) The role of nanomaterials in translational medicine. ACS Nano 5(5):3419–3424

Lee JH, Kim DO et al (2007) Direct metallization of gold nanoparticles on a polystyrene bead surface using cationic gold ligands. Macromol Rapid Commun 28(5):634–640

Lee EP, Peng Z et al (2008) Electrocatalytic properties of Pt nanowires supported on Pt and W gauzes. ACS Nano 2(10):2167–2173

Malloy A, Carr B (2006) NanoParticle tracking analysis—the Halo™ System. Part Part Syst Charact 23(2):197–204

Radziuk D, Grigoriev D et al (2010) Ultrasound-assisted fusion of preformed gold nanoparticles. J Phys Chem C 114(4): 1835–1843

Schellekens H (2002) Bioequivalence and the immunogenicity of biopharmaceuticals. Nat Rev Drug Discov 1(6):457–462

Sekhon BS, Kamboj SR (2010) Inorganic nanomedicine—part 2. Nanomed Nanotechnol Biol Med 6(5):612–618

Sungchul J, Daniel FB (2010) Adhesion mechanisms of nanoparticle silver to substrate materials: identification. Nanotechnology 21(5):055204

Takayasu MM, Galembeck F (1998) Determination of the equivalent radii and fractal dimension of polystyrene latex aggregates from sedimentation coefficients. J Colloid Interf Sci 202(1):84–88

Tian J, Jin J et al (2010) Self-assembly of gold nanoparticles and polystyrene: a highly versatile approach to the preparation of colloidal particles with polystyrene cores and gold nanoparticle coronae. Langmuir 26(11):8762–8768

Tian J, Zheng F et al (2011) Self-assembly of polystyrene with pendant hydrophilic gold nanoparticles: the influence of the hydrophilicity of the hybrid polymers. J Mater Chem 21(42):16928–16934

Zhong Z, Chen F et al (2006) Assembly of Au colloids into linear and spherical aggregates and effect of ultrasound irradiation on structure. J Mater Chem 16(5):489–495

Zhou J, Ralston J et al (2009) Functionalized gold nanoparticles: synthesis, structure and colloid stability. J Colloid Interf Sci 331(2):251–262